

See discussions, stats, and author profiles for this publication at: <https://www.researchgate.net/publication/47659452>

Highly Resolved Online Organic–Chemical Speciation of Evolved Gases from Thermal Analysis Devices by Cryogenically Modulated Fast Gas Chromatography Coupled to Single Photon Ioniza...

ARTICLE *in* ANALYTICAL CHEMISTRY · NOVEMBER 2010

Impact Factor: 5.64 · DOI: 10.1021/ac100745h · Source: PubMed

CITATIONS

13

READS

33

8 AUTHORS, INCLUDING:



Mohammad Reza Saraji-Bozorgzad

Helmholtz Zentrum München

19 PUBLICATIONS 269 CITATIONS

[SEE PROFILE](#)



Markus Eschner

14 PUBLICATIONS 144 CITATIONS

[SEE PROFILE](#)



Thomas Gröger

Helmholtz Zentrum München

47 PUBLICATIONS 345 CITATIONS

[SEE PROFILE](#)

Highly Resolved Online Organic-Chemical Speciation of Evolved Gases from Thermal Analysis Devices by Cryogenically Modulated Fast Gas Chromatography Coupled to Single Photon Ionization Mass Spectrometry

Mohammad R. Saraji-Bozorgzad,[†] Markus Eschner,[‡] Thomas M. Groeger,[†] Thorsten Streibel,[§] Robert Geissler,[†] Erwin Kaisersberger,^{||} Thomas Denner,^{||} and Ralf Zimmermann^{*,†,§}

Helmholtz Zentrum München, Institut für Ökologische Chemie, Deutsches Forschungszentrum für Gesundheit und Umwelt (GmbH), D-85764 Neuherberg, Germany, Universität Augsburg, D-86167 Augsburg, Germany, Institut für Chemie, Lehrstuhl für Analytische Chemie, Abteilung für Analytische, Technische und Umweltchemie, Universität Rostock, D-18059 Rostock, Germany, and Netzsch-Gerätebau GmbH, D-95100 Selb, Germany

Multi-dimensional analysis (MDA) in analytical chemistry is often applied to improve the selectivity of an analytical device and, therefore, to achieve a better overview of a sample composition. Recently, the hyphenation of thermogravimetry with single photo ionization mass spectrometry (TG-SPIMS) using an electron beam pumped excimer lamp (EBEL) for VUV radiation was applied. The concept of MDA has been realized by upgrading the TG-SPIMS system with a quasi comprehensive chromatographic separation step before the soft ionization (TG-GCxSPIMS). The system was characterized by the thermal analysis of diesel fuel, which has often been investigated by the GCxGC-community and is therefore a well-known sample material in MDA. Data from this measurement are used to explain the three-dimensional data structure and the advantages of the online TG-GCxSPIMS as compared to TG-SPIMS. Subsequently, the thermal decomposition behavior of a polymer, acrylonitrile-butadiene-styrene (ABS), is investigated. TG-GCxSPIMS provides a two-dimensional analysis of the evolved gaseous products. TG relevant data are obtained as well as an improved resolution power to separate isobaric molecular structures without losing any fraction of the samples, as is often the case in heart cutting approaches. Additionally, this solution is not associated with any extension of the measurement time. The assignment of the substance pattern to distinct species is improved as compared to solely using mass spectrometry without a preceding separation step. Furthermore, hitherto undetected compounds have been found in the evolved gases from the thermal degradation of ABS. Finally, a first estimation of the limit of detection has been carried out. This results in a significant decrease

of the LOD in case of TG-GCxSPIMS (500 ppt for toluene) as compared to 30 ppb, which could be reached with TG-SPIMS.

Thermal analysis (TA) comprises a group of techniques that is performed on samples to determine changes in their physical properties as a function of temperature, in relation to a temperature program. For many research and industrial applications, the information obtained from the thermogravimetry (TG) curve (sample mass vs temperature curve) or the derivative TG curve (DTG, first derivative of sample mass vs temperature curve) as well as the enthalpy (differential scanning calorimetry (DSC) curve) is used for, for example, quality control or advanced material research.^{1–8} These parameters are needed to characterize temperature-dependent material properties, to evaluate thermodynamical conversions and thermophysical parameters, as well as to observe chemical reactions. Because of thermal stress, the samples undergo chemical and physical alteration, which is often related to an enthalpy change or the evolving of gaseous components. This is often measured with TA techniques such as TG and DSC. However, for a more detailed and advanced investigation, for example, identification of the gaseous compounds evolving during TA application, often a chemical detection technique is indispensable.⁹ Evolved gas analysis (EGA) is applied, if the detection technique offers both identification and quantification of the gaseous compounds. Depending on the requirements,

- (1) Fatu, D.; Geambas, G.; Segal, E.; Budrugeac, P.; Ciutacu, S. *Thermochim. Acta* **1989**, *149*, 181–187.
- (2) Sourour, S.; Kamal, M. R. *Thermochim. Acta* **1976**, *14*, 41–59.
- (3) Asalettha, R.; Kumaran, M. G.; Thomas, S. *Polym. Degrad. Stab.* **1998**, *61*, 431–439.
- (4) Covolan, V. L.; Fernandes, E. G.; D'Antone, S.; Chiellini, E. *Thermochim. Acta* **1999**, *342*, 97–103.
- (5) Li, Y.; Fan, Y.; Ma, J. *Polym. Degrad. Stab.* **2001**, *73*, 163–167.
- (6) Stack, S.; O'Donoghue, O.; Birkinshaw, C. *Polym. Degrad. Stab.* **2003**, *79*, 29–36.
- (7) Faravelli, T.; Bozzano, G.; Scassa, C.; Perego, M.; Fabini, S.; Ranzi, E.; Dente, M. *J. Anal. Appl. Pyrolysis* **1999**, *52*, 87–103.
- (8) Yang, J.; Miranda, R.; Roy, C. *Polym. Degrad. Stab.* **2001**, *73*, 455–461.
- (9) Raemakers, K. G. H.; Bart, J. C. J. *Thermochim. Acta* **1997**, *295*, 1–58.

* To whom correspondence should be addressed. E-mail: ralf.zimmermann@helmholtz-muenchen.de.

[†] Deutsches Forschungszentrum für Gesundheit und Umwelt (GmbH).

[‡] Universität Augsburg.

[§] Universität Rostock.

^{||} Netzsch-Gerätebau GmbH.

EGA can be realized by offline coupling of TG with sequentially working analytical techniques such as gas chromatography (GC)^{10–12} or with online real-time detection such as Fourier transform infrared spectroscopy (FT-IR)¹³ or mass spectrometry (MS).^{14–16} FT-IR is a very powerful tool for chemical group investigation; however, it has difficulties distinguishing between molecular substances, and, therefore, TG-MS has become the most common available hyphenation. The hyphenation between TG and MS can be carried out either by a capillary coupling¹⁷ or with a skinned super sonic expansion device.¹⁸ Most often, inexpensive quadrupole mass spectrometers (QMS) are coupled to TG. In most cases, electron ionization (EI) is applied. Depending on the chemical class of the molecule and the used kinetic energy of the electrons, most EI mass spectra hardly contain molecular ion signals. Because of the high excess energy, the spectra are dominated by fragment peaks. Some of these fragment signals are characteristic of specific classes of molecules or functional groups. Therefore, they can be used for identification by comparing sample spectra against reference spectra (e.g., NIST spectra library). However, in case of overlapping signals, identification and quantification could become very complicated or even impossible. To overcome this problem, different approaches have been developed by several research groups in the past forty years. One auspicious method is represented by using soft ionization methods, where fragmentation of organic molecules from EGA can be circumvented. Depending on the analytical problem, interfaces allowing soft ionization are utilized such as chemical ionization (CI),¹⁹ field ionization (FI),²⁰ meta stable atom bombardment (MAB),^{21–24} which is based on Penning ionization,²⁵ and photo ionization (PI).^{26–33} MS with soft ionization provides mass spectra, which in most cases only show molecular ion peaks [M⁺]. These mass spectra thus contain less peaks and are

- (10) Chiu, J. *Anal. Chem.* **1968**, *40*, 1516–1520.
- (11) Tsuge, S.; Sugimura, Y.; Nagaya, T. *J. Anal. Appl. Pyrolysis* **1980**, *1*, 221–229.
- (12) Costa, L.; Camino, G.; Trossarelli, L. *J. Anal. Appl. Pyrolysis* **1985**, *8*, 15–24.
- (13) Herrera, M.; Wilhelm, M.; Matuschek, G.; Kettrup, A. *J. Anal. Appl. Pyrolysis* **2001**, *58*–59, 173–188.
- (14) Chiu, J.; Beattie, A. J. *Thermochim. Acta* **1980**, *40*, 251–259.
- (15) Chiu, J.; Beattie, A. J. *Thermochim. Acta* **1981**, *50*, 49–56.
- (16) Maciejewski, M.; Baiker, A. *Thermochim. Acta* **1997**, *295*, 95–105.
- (17) Kaisersberger, E.; Post, E. *Thermochim. Acta* **1997**, *295*, 73–93.
- (18) Kaisersberger, E.; Post, E. *Thermochim. Acta* **1998**, *324*, 197–201.
- (19) Baumgartner, E.; Nachbaur, E. *Thermochim. Acta* **1977**, *19*, 3–12.
- (20) Yun, Y.; Meuzelaar, H. L. C.; Simmleit, N.; Schulten, H. R. *Energy Fuels* **1991**, *5*, 22–29.
- (21) Faubert, D.; Paul, G. J. C.; Giroux, J.; Bertrand, M. *J. Int. J. Mass Spectrom. Ion Processes* **1993**, *124*, 69–77.
- (22) Moore, S. *Chemosphere* **2002**, *49*, 121–125.
- (23) Boutin, M.; Lesage, J.; Ostiguy, C.; Bertrand, M. *J. J. Anal. Appl. Pyrolysis* **2003**, *70*, 505–517.
- (24) Boutin, M.; Lesage, J.; Ostiguy, C.; Bertrand, M. *J. J. Am. Soc. Mass Spectrom.* **2004**, *15*, 1315–1319.
- (25) Madison, T. A.; Siska, P. E. *J. Chem. Phys.* **2009**, *131*, 134309–134309.
- (26) Butcher, D. J. *Microchem. J.* **1999**, *62*, 354–362.
- (27) Streibel, T.; Adam, T.; Mitschke, S.; Cao, L.; Mühlberger, F.; Zimmermann, R. Alicante, Spain, 2004; p 63.
- (28) Streibel, T.; Geissler, R.; Saraji-Bozorgzad, M.; Sklorz, M.; Kaisersberger, E.; Denner, T.; Zimmermann, R. *J. Therm. Anal. Calorim.* **2009**, *96*, 795–804.
- (29) Hanley, L.; Zimmermann, R. *Anal. Chem.* **2009**, *81*, 4174–4182.
- (30) Boesl, U.; Neusser, H. J.; Schlag, E. W. *Chem. Phys.* **1981**, *55*, 193–204.
- (31) Boesl, U.; Zimmermann, R.; Weickhardt, C.; Lenoir, D.; Schramm, K.-W.; Kettrup, A.; Schlag, E. W. *Chemosphere* **1994**, *29*, 1429–1440.
- (32) Streibel, T.; Hafner, K.; Mühlberger, F.; Adam, T.; Zimmermann, R. *Appl. Spectrosc.* **2006**, *60*, 72–79.
- (33) Geissler, R.; Saraji-Bozorgzad, M. R.; Groeger, T.; Fendt, A.; Streibel, T.; Sklorz, M.; Krooss, B. M.; Fuhrer, K.; Gonin, M.; Kaisersberger, E.; Denner, T.; Zimmermann, R. *Anal. Chem.* **2009**, *81*, 6038–6048.
- (34) Zoller, D. L.; Johnston, M. V.; Tomic, J.; Wang, X.; Calkins, W. H. *Energy Fuels* **1999**, *13*, 1097–1104.
- (35) Zoller, D. L.; Sum, S. T.; Johnston, M. V. *Anal. Chem.* **1999**, *71*, 866–872.
- (36) Adam, T.; Streibel, T.; Mitschke, S.; Mühlberger, F.; Baker, R. R.; Zimmermann, R. *J. Anal. Appl. Pyrolysis* **2005**, *74*, 454–464.
- (37) Adam, T.; Mühlberger, F.; Mitschke, S. Norfolk, VA, 2003.
- (38) Arii, T.; Otake, S.; Takata, Y.; Matsuura, S. *J. Mass Spectrom. Soc. Jpn.* **2006**, *54*, 243–249.
- (39) Arii, T.; Otake, S. *J. Therm. Anal. Calorim.* **2007**, *91*, 419–426.
- (40) Saraji-Bozorgzad, M.; Geissler, R.; Streibel, T.; Mühlberger, F.; Sklorz, M.; Kaisersberger, E.; Denner, T.; Zimmermann, R. *Anal. Chem.* **2008**, *80*, 3393–3403.
- (41) Saraji-Bozorgzad, M.; Geissler, R.; Streibel, T.; Sklorz, M.; Kaisersberger, E.; Denner, T.; Zimmermann, R. *J. Therm. Anal. Calorim.* **2009**, *97*, 689–694.
- (42) Zimmermann, R.; Lenoir, D.; Schramm, K.-W.; Kettrup, A.; Boesl, U. *Organohalogen Compd.* **1994**, *19*, 155–160.
- (43) Zimmermann, R.; Lermer, C.; Lenoir, D.; Boesl, U. *Bernkastel-Kues*; American Institute of Physics, AIP-Press: New York, 1995; pp 527–530.
- (44) Zimmermann, R.; Lermer, C.; Schramm, K.-W.; Kettrup, A.; Boesl, U. *Eur. Mass Spectrom.* **1995**, *1*, 341–351.
- (45) Day, M.; Cooney, J. D.; Touchette-Barrette, C.; Sheehan, S. E. *J. Anal. Appl. Pyrolysis* **1999**, *52*, 199–224.
- (46) Jakab, E.; Blazso, M. *J. Anal. Appl. Pyrolysis* **2002**, *64*, 263–277.

therefore clear and easy to interpret, even in case of substance mixtures, which would not be the case with EI-MS. Boutin et al.²⁴ used temperature-programmed pyrolyzer coupled with MAB-MS (TPPy/MAB-MS) for the identification of additives in polymers. First thermal decomposition measurements and pyrolysis studies using laser-based photon ionization have been carried out by others and our own research group.^{34–37} As laser-based instrumentation often involves big drawbacks, regarding the high costs and complexity of the laser devices, VUV lamps such as deuterium or krypton discharge and electron beam pumped excimer light source (EBEL) are an attractive option. Arri et al. reported on the coupling of TG-PIMS using deuterium discharge lamps and QMS to investigate the behavior of polymer decomposition.^{38,39} The hyphenation of a thermo balance with QMS as well as an orthogonal-acceleration time-of-flight mass spectrometry (oa-TOFMS) for the assay of plastics and crude oil samples using an EBEL as photon source has also been reported in the past.^{33,40,41} In case of single photon ionization (SPI), only one photon with the energy E_{hv} higher than the ionization energy E_i of the relevant molecule can lead to ionization. Consequently, the photon energy determines selectivity and acts as an energetic threshold. Molecules with an $E_i < E_{hv}$ can be ionized without any regard to their chemical composition and structure in contrast to resonance enhanced multi photon ionization (REMPI), which is known as a selective ionization method.^{42–44} Although SPI mass spectra mainly consist of molecular ion peaks, a correlation between mass information and molecular structure is impossible, if there is no information about the sample composition. Therefore, SPI as a quasi selective ionization method is not suited to differ between isobaric (molecules of different classes with the same nominal mass) or isomeric (molecules of the same class with different molecular structure) molecules.

Besides soft ionization methods, another promising way to ease the investigation of complex sample mixtures is the coupling of thermal analysis (TA) with a separation technique, for example GC, in combination with MS (TG-GC/MS, Py-GC/MS, and TD/TE-GC/MS).^{45–50} Because of different retention behaviors, the evolved compounds from the sample reach the ion source of

- (33) Geissler, R.; Saraji-Bozorgzad, M. R.; Groeger, T.; Fendt, A.; Streibel, T.; Sklorz, M.; Krooss, B. M.; Fuhrer, K.; Gonin, M.; Kaisersberger, E.; Denner, T.; Zimmermann, R. *Anal. Chem.* **2009**, *81*, 6038–6048.
- (34) Zoller, D. L.; Johnston, M. V.; Tomic, J.; Wang, X.; Calkins, W. H. *Energy Fuels* **1999**, *13*, 1097–1104.
- (35) Zoller, D. L.; Sum, S. T.; Johnston, M. V. *Anal. Chem.* **1999**, *71*, 866–872.
- (36) Adam, T.; Streibel, T.; Mitschke, S.; Mühlberger, F.; Baker, R. R.; Zimmermann, R. *J. Anal. Appl. Pyrolysis* **2005**, *74*, 454–464.
- (37) Adam, T.; Mühlberger, F.; Mitschke, S. Norfolk, VA, 2003.
- (38) Arii, T.; Otake, S.; Takata, Y.; Matsuura, S. *J. Mass Spectrom. Soc. Jpn.* **2006**, *54*, 243–249.
- (39) Arii, T.; Otake, S. *J. Therm. Anal. Calorim.* **2007**, *91*, 419–426.
- (40) Saraji-Bozorgzad, M.; Geissler, R.; Streibel, T.; Mühlberger, F.; Sklorz, M.; Kaisersberger, E.; Denner, T.; Zimmermann, R. *Anal. Chem.* **2008**, *80*, 3393–3403.
- (41) Saraji-Bozorgzad, M.; Geissler, R.; Streibel, T.; Sklorz, M.; Kaisersberger, E.; Denner, T.; Zimmermann, R. *J. Therm. Anal. Calorim.* **2009**, *97*, 689–694.
- (42) Zimmermann, R.; Lenoir, D.; Schramm, K.-W.; Kettrup, A.; Boesl, U. *Organohalogen Compd.* **1994**, *19*, 155–160.
- (43) Zimmermann, R.; Lermer, C.; Lenoir, D.; Boesl, U. *Bernkastel-Kues*; American Institute of Physics, AIP-Press: New York, 1995; pp 527–530.
- (44) Zimmermann, R.; Lermer, C.; Schramm, K.-W.; Kettrup, A.; Boesl, U. *Eur. Mass Spectrom.* **1995**, *1*, 341–351.
- (45) Day, M.; Cooney, J. D.; Touchette-Barrette, C.; Sheehan, S. E. *J. Anal. Appl. Pyrolysis* **1999**, *52*, 199–224.
- (46) Jakab, E.; Blazso, M. *J. Anal. Appl. Pyrolysis* **2002**, *64*, 263–277.

the MS at different times. Consequently, the number of simultaneously ionized compounds is reduced. Thus, even in case of EI, mass spectra become easier to interpret as the number of overlapped signals is reduced. Examples for these couplings are Py-GC/MS and TG-GC/MS. For an online connection of the TA with the GC, samples have to be focused before they are injected to the GC. This can be done either by an instant evaporation of the sample as is the case in the injector of the GC or by collecting the sample in so-called cold traps (CT) and releasing them by raising the temperature again. In case of Py-GC/MS, samples can be pyrolyzed instantly (flash pyrolysis), and often a narrow plug is transferred to the GC/MS. Therefore, all of the evolved gases can be separated within only one GC run. Here, the pyrolyzer acts as an injector. This method, however, does not provide physically relevant parameters (e.g., mass loss or reaction enthalpy of the sample). Furthermore, in case of flash pyrolysis, the reaction kinetics can extremely differ from a continuously heated analysis of the sample. TA-GC/MS in contrast to Py-GC/MS offers TG, DTG, and DSC signals, but its drawback is based on the offline character of the GC technique. To analyze the continuously released gases from the TA with an offline analytical device, they have to be collected and analyzed subsequently. This is associated with sample preparation and longer measurement periods, and, additionally, chemical reactions between products are not to be excluded upon subsequent sample handling (heating). An online coupling of the TG-GC/MS can be realized using valve systems in combination with sample loops allowing a quasi continuous operation of the TG-GC/MS system.^{51–53} These systems can uniquely be used for high performance qualitative and quantitative EGA. However, a prior knowledge of the sample is indispensable, and, moreover, only parts of the molecular composition are usually analyzed, while sample information during two GC runs gets lost (heart cut technique).

Up to now, only conventionally used chromatographic separation techniques are discussed to overcome the problems of co-ionized sample compounds. However, if an online hyphenation of TA with MS as well as isobaric or isomeric separation is required, multi-dimensional analysis may become promising.

Multi-Dimensional Analysis (MDA). To improve the selectivity of an analytical device and, therefore, to achieve a better overview about a sample composition, two or more independent separating methods can be coupled inline. One of the widespread MDA techniques is multi-dimensional separation using two-dimensional GC (GC-GC or GCxGC), where GC-GC represents the heart cut technique. Here, two different chromatographic capillaries are connected serially. Often valve systems are utilized between the two columns to transfer fractions of interest and lead them to the second column for further separation. GCxGC in contrast to GC-GC uses modulators and normally a shorter second

GC capillary. The modulator acts as a device connected between the first and the second GC column to focus and to reinject the eluents from the first into the second column. Therefore, the eluents from the first column are trapped for a short time interval, that is, modulation period, and then released into the second column. The functionality and the different types of modulators used for GCxGC have been described in detail in literature.^{54–58} The choice of the second column parameters (its length, inner diameter, phase, and film thickness) as well as the modulator type and modulation time are thereby crucial.

As described earlier, SPIMS with its soft ionization character could also act as a separation technique. This holds for the ideal case, if the relation between analyte and ions becomes biunique. It has been demonstrated that gas chromatography-single photon ionization mass spectrometry (GCxSPIMS)⁵⁴ resembles GCxGC closely in its essential principles. In both cases, sample components undergo a first separation in time by GC, and small fractions of the eluate are led subsequently to the secondary analytical device either individually or at least in greatly simplified submixtures. Where the first GC creates a primary retention time axis, the second instrument with its own resolving power operates as a detector for the inlet GC and provides an independent analysis of the dispersed sample eluting from the primary GC.⁵⁴ The second instrument provides an additional separation of these small fractions depending on the molecular mass (SPIMS), respectively, the retention behavior (GC). GCxGC as well as GCxSPIMS combine independent analytical techniques and generate comprehensive two-dimensional data sets. In case of GCxGC, the two dimensions are given by two different retention time axes, and each substance is defined by its specific location in the separation plane. This holds also for GCxSPIMS, where the separated compounds are determined by their retention time in the first and the corresponding molecular mass to charge ratio of each component (m/z) in the second. For a more detailed analysis, further methods can be hyphenated to each other. Examples therefore, such as GCxGCxSPIMS,⁵⁹ liquid chromatography (LC) coupled to GCxMS (LC-GCxMS),^{60,61} and other combinations (GCxGCxGC) are given in the literature.^{62,63} With each additional application, the selectivity of the system will increase, and the data set extends by one further separation dimension. However, it is a challenge to keep the complexity of the apparatus low and to provide that, after each separation, the entirety of the eluents is led to the next separation step without merging.

- (47) Herrera, M.; Matuschek, G.; Kettrup, A. *J. Anal. Appl. Pyrolysis* **2003**, *70*, 35–42.
- (48) Bozi, J.; Czegeny, Z.; Meszaros, E.; Blazso, M. *J. Anal. Appl. Pyrolysis* **2007**, *79*, 337–345.
- (49) Ho, S. S. H.; Yu, J. Z. *J. Chromatogr., A* **2004**, *1059*, 121–129.
- (50) Ho, S. S. H.; Yu, J. Z.; Chow, J. C.; Zielinska, B.; Watson, J. G.; Sit, E. H. L.; Schauer, J. *J. Chromatogr., A* **2008**, *1200*, 217–227.
- (51) Egger, P.; Dire, S.; Ischia, M.; Campostrini, R. *J. Therm. Anal. Calorim.* **2005**, *81*, 407–415.
- (52) Ischia, M.; Perazzoli, C.; Dal Maschio, R.; Campostrini, R. *J. Therm. Anal. Calorim.* **2007**, *87*, 567–574.
- (53) Howell, B. A. *J. Therm. Anal. Calorim.* **2007**, *89*, 393–398.
- (54) Phillips, J. B.; Xu, J. *J. Chromatogr., A* **1995**, *703*, 327–334.
- (55) Adahchour, M.; Beens, J.; Vreuls, R. J. J.; Brinkman, U. A. T. *TrAC, Trends Anal. Chem.* **2006**, *25*, 438–454.
- (56) Adahchour, M.; Beens, J.; Vreuls, R. J. J.; Brinkman, U. A. T. *TrAC, Trends Anal. Chem.* **2006**, *25*, 540–553.
- (57) Adahchour, M.; Beens, J.; Vreuls, R. J. J.; Brinkman, U. A. T. *TrAC, Trends Anal. Chem.* **2006**, *25*, 726–741.
- (58) Adahchour, M.; Beens, J.; Vreuls, R. J. J.; Brinkman, U. A. T. *TrAC, Trends Anal. Chem.* **2006**, *25*, 821–840.
- (59) Welthagen, W.; Mitschke, S.; Muhlberger, F.; Zimmermann, R. *J. Chromatogr., A* **2007**, *1150*, 54–61.
- (60) Edam, R.; Blomberg, J.; Janssen, H. G.; Schoenmakers, P. J. *J. Chromatogr., A* **2005**, *1086*, 12–20.
- (61) Biedermann, M.; Grob, K. *J. Sep. Sci.* **2009**, *32*, 3726–3737.
- (62) Ledford, E. B.; Billesbach, C. A.; Zhu, Q. Y. *J. High Resolut. Chromatogr.* **2000**, *23*, 205–207.
- (63) Watson, N. E.; Siegler, W. C.; Hoggard, J. C.; Synovec, R. E. *Anal. Chem.* **2007**, *79*, 8270–8280.

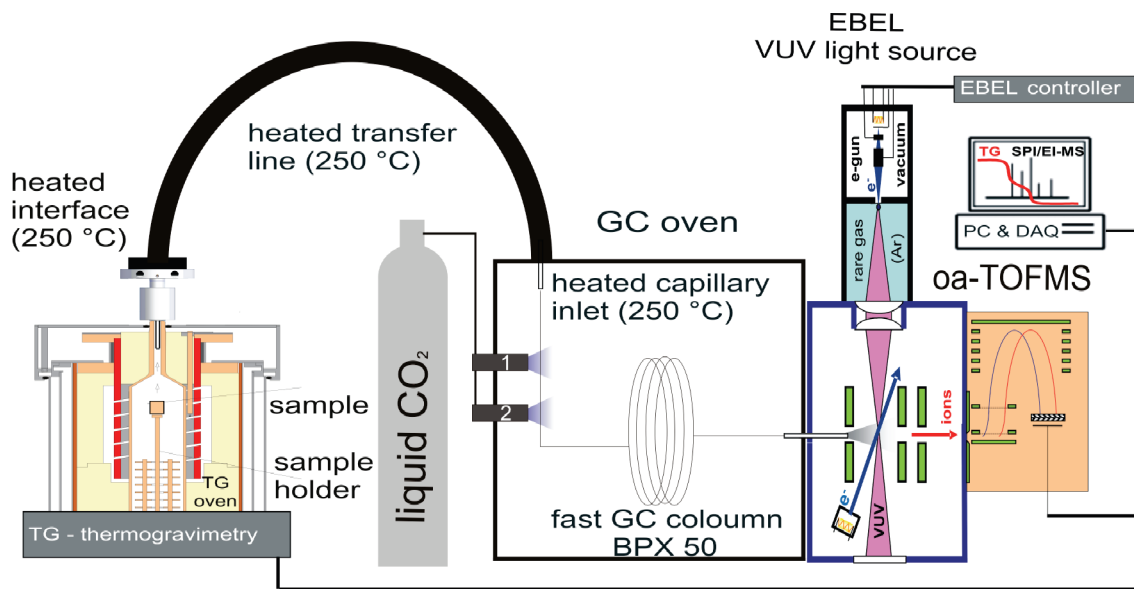


Figure 1. Schematic drawing of the TG-GCxSPIMS system.

Recently, we adapted the concept of MDA to TA by applying TG-SPIMS.³³ Now we upgraded this system and included also a quasi comprehensive chromatographic separation step before soft ionization (TG-GCxSPIMS). For the investigation of samples such as diesel fuel and polymer blends, a thermo balance was connected to a GCxSPIMS system using a modulator to chop, trap, refocus, and reinject the continuous evolved gas stream from the TG system into the GCxSPIMS device as it is explained in detail in the next section.

Instrumentation and Experimental Setup. For the thermal degradation and decomposition, a STA 409 PG Luxx thermo balance (Netzsch Geraetebau GmbH, Selb, Germany) was applied. The samples were heated in an Al₂O₃ crucible from ambient temperature of the furnace (40 °C) to 1000 °C with a heating rate of 10 K min⁻¹ in an N₂ atmosphere (column flow = 1.4 mL/min). During all measurements, the gas flow through the STA was set to 60 mL/min. A heated transfer line (Horst GmbH, Lorsch, Germany) enclosing a deactivated fused silica capillary (2.5 m × 250 μm i.d.) connected the thermo balance with a GC (Thermo Trace GCxGC, Thermo Fisher Scientific Inc.). The GC oven is equipped with a two stage liquid CO₂ spray modulator for GCxGC measurements. The injection system of the GC system was not used and disconnected from the gas flow. For our TG-GCxSPIMS experiments, the fused silica transfer capillary from TG was further connected to a BPX 50 GC column (3 m × 250 μm, 0.25 μm, 50% phenyl polysilphenylene-siloxane film, GSE) and was guided through the column holder of the modulator close to the modulator nozzles as pictured schematically in Figure 1. During one modulation cycle (30 s), the GC column is cooled by the CO₂ stream approximately to -69 °C at the second stage, while the first CO₂ spray is turned off. The eluents are trapped at this cold spot and can be concentrated, while the carrier gas (N₂) sustains the gas flow to the MS. After 15 s, the first stage turns on, stops the flow of the sample substances, and the second stage turns off. The trapped samples at the second stage become mobilized again due to the temperature of the GC oven and can be separated by the GC column, before they are guided

through the gas inlet system into the MS. The gas inlet system is based on a completely heated 30 cm long aluminum cylinder acting as a short transfer line between the GC oven and the ion source of the MS. The GC capillary was inserting into the vacuum chamber through a heated steel needle in center of the inlet interface, and it was positioned close to an opening of the ion chamber. The oaTOFMS extraction rate was set to 65 kHz. For TG-GCxSPIMS experiments, 6500 single extractions (data acquisition frequency = 10 Hz), and for TG-SPIMS measurements 65 000 (data acquisition frequency = 1 Hz) transient extractions were averaged to a mass spectrum by an analogue-to-digital conversion data acquisition card (model DP 240, Acciris, Geneva, Switzerland) and recorded to the hard disk of a personal computer.

For photo ionization, VUV light with a center wavelength of 126 nm (9.8 eV) was generated by a self-made electron beam pumped excimer light source (EBEL). The interface as well as detailed information about the EBEL are given elsewhere.^{64–66}

RESULTS AND DISCUSSION

The system was characterized by the thermal analysis of diesel fuel, which is a well-known and often investigated sample in the GCxGC community and, therefore, a well-suited sample material for characterization of this MDA device. Data from this measurement are used to explain the three-dimensional data structure and the advantages of the online TG-GCxSPIMS as compared to TG-SPIMS. For comparison purposes, the diesel sample was further investigated by GCxSPIMS and GCxGC-EIMS. The latter technique was used to unravel the molecular structures of the separated species. Subsequently, the thermal decomposition behavior of a polymer, acrylonitrile-butadiene-styrene, is investigated.

Comparison between TG-SPIMS and TG-GCxSPIMS. The hyphenations of TG-EBEL-QMS and TG-EBEL-oaTOFMS

- (64) Mühlberger, F.; Wieser, J.; Morozov, A.; Ulrich, A.; Zimmermann, R. *Anal. Chem.* **2005**, *77*, 2218–2226.
- (65) Mühlberger, F.; Saraji-Bozorgzad, M.; Gonin, M.; Fuhrer, K.; Zimmermann, R. *Anal. Chem.* **2007**, *79*, 8118–8124.
- (66) Mühlberger, F.; Streibel, T.; Wieser, J.; Ulrich, A.; Zimmermann, R. *Anal. Chem.* **2005**, *77*, 7408–7414.

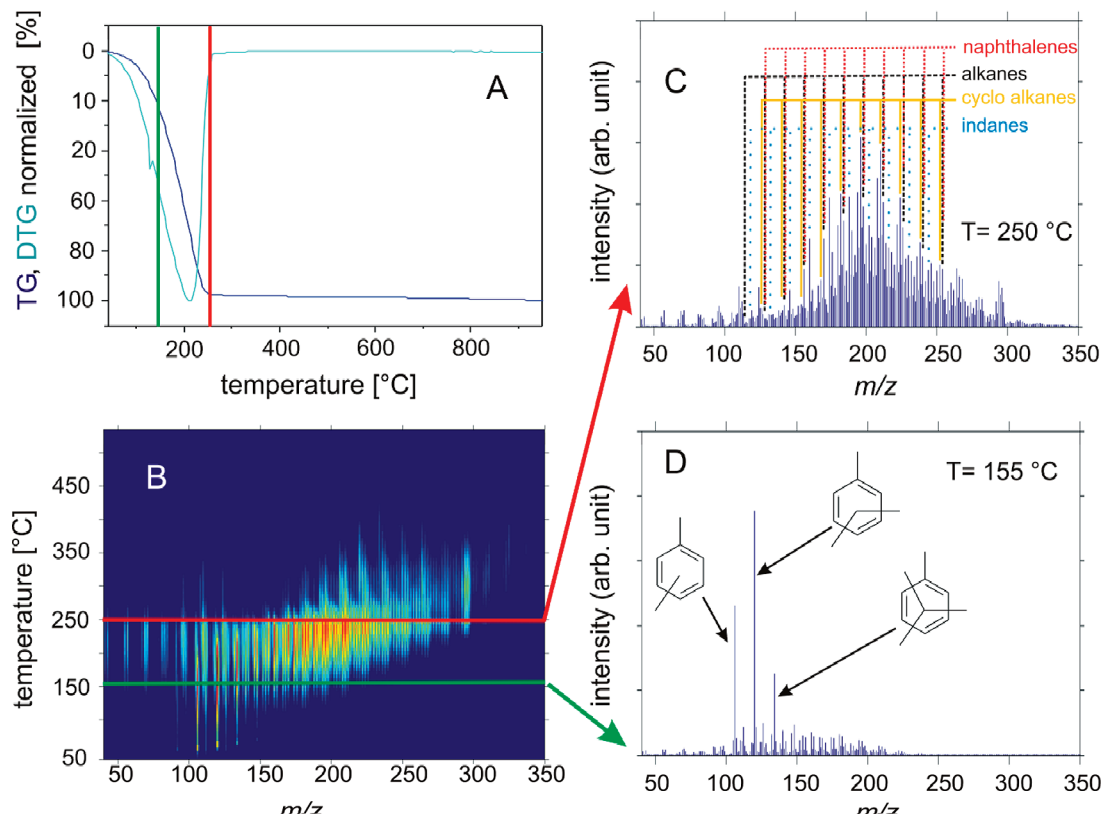


Figure 2. (A) TG and DTG curves of diesel fuel sample. (B) TG-SPIMS results forming a 2D color-coded intensity plot of TG oven temperature versus m/z . (C) SPI-TOFMS spectrum at $T = 250$ °C. (D) SPI-TOFMS spectrum at $T = 155$ °C.

systems have already been reported.^{33,40,41,67} The results of a diesel fuel measurement, forming a two-dimensional color-coded intensity contour plot with the axes X (m/z) and Y (temperature of the TG-furnace), are shown in Figure 2B. For demonstration, two mass spectra (Figure 2C and D), which provide a simplified picture of the composition of the evolved gases from the thermo balance at different temperatures, are depicted. The SPI spectrum at 155 °C (green) is dominated by C_2 -, C_3 -, and C_4 -alkylated benzene species (ranging from a total number of substituted C atoms from two to four), whereas the SPI spectrum at 250 °C is dominated by the homologous series of alkanes, cycloalkanes, indanes, and naphthalenes. Here, isobaric compounds, such as nonane ($m/z = 128.17$) and naphthalene ($m/z = 128.26$) and their homologues, cannot be distinguished due to the moderate resolving power of the compact oaTOFMS, which is in the range of approximately 850 ($m/\Delta m_{\text{fwhm}}$). Therefore, neither unambiguous identification nor quantification can be provided.

For a closer inspection, the ion traces of $m/z = 128$ provided by both TG-SPIMS and TG-GCxSPIMS are displayed in Figure 3. Figure 3A shows the super positioned ion traces of naphthalene and nonane as it is provided by TG-SPIMS. TG-GCxSPIMS, in contrast, pictures clearly two modulated ion traces with two maxima at different temperatures due to the separation by the added GC unit. The rectangular box in (A) and (B) represents a time interval of 30 s, which is as long as one modulation cycle (D) and equal to a temperature window of 5 °C. Three ion traces,

$m/z = 106$, $m/z = 128$, and $m/z = 142$, are shown in Figure 3C–E. As it is well-known for BPX50 columns, ethyl benzene, m -xylene, and p -xylene show a quite similar retention behavior, which, depending on the column lengths, can lead to coelution of these compounds. In contrast, the retention time of o -xylene differs clearly. The two peaks in Figure 3C are overlapping signals of ethyl benzene, m -xylene, and p -xylene, with the second peak corresponding to o -xylene. This could also be observed by investigating the diesel sample with GCxGCxEIMS and by subsequent measurements of a mixture of ethyl benzene, m -xylene, p -xylene, and o -xylene by a GCxSPIMS device. Figure 3C is an example of an isomeric separation, which in contrast to isobaric separation cannot be reached, even when high resolution mass spectrometry (HRMS), for example, FTICR-MS is used. In Figure 3D, the ion traces of the two molecules with $m/z = 128$ are demonstrated. It represents a clear separation of these two isobaric compounds. The two peaks during one modulation cycle can be attributed to nonane (black dot) and naphthalene (red dot). To verify this positioning, the different boiling points according to the NIST database are used. Nonane ($T_{\text{boiling}} = 150$ °C) volatilizes earlier as compared to naphthalene and shows a decreasing intensity course, whereas naphthalene ($T_{\text{boiling}} = 217$ °C) exhibits an increasing signal intensity at the same time. Additionally, comparisons to Figure 3E containing the ion traces of decane ($m/z = 142$, black dot) and two C_2 -alkylated naphthalenes ($m/z = 142$, red dots) can lead to the same conclusion. The retention times of the two alkanes are almost similar due to their unpolar nature, whereas naphthalene and C_2 -alkylated naphthalene show a higher dislocation because of their differ-

(67) Geissler, R.; Saraji-Bozorgzad, M.; Streibel, T.; Kaisersberger, E.; Denner, T.; Zimmermann, R. *J. Therm. Anal. Calorim.* 2009, 96, 813–820.

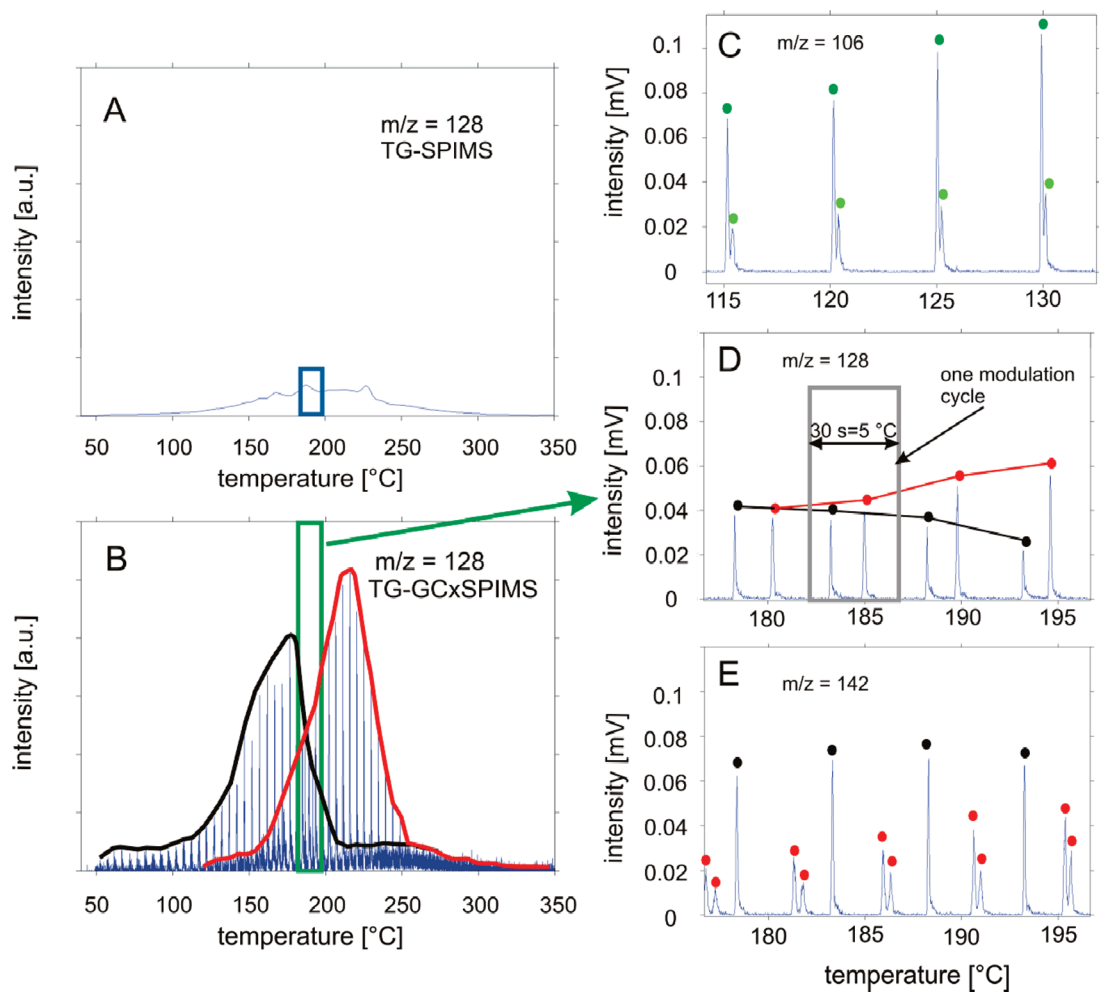


Figure 3. (A) Ion trace of $m/z = 128$ as a function of TG oven temperature measured with TG-SPIMS. (B) Ion trace of $m/z = 128$ as a function of TG oven temperature measured with TG-GCxSPIMS. (C) Ion trace of $m/z = 106$ measured with TG-GCxSPIMS demonstrating an isomeric separation. (D,E) Ion trace of $m/z = 128$ and $m/z = 142$, respectively, measured with TG-GCxSPIMS demonstrating an isobaric separation.

ences in polarity. Because of the retention behavior of the sample compounds, isobaric as well as isomeric molecular structures can be separated, and, therefore, not only identification, but additional quantification can be provided.

In addition to the improved resolving power of the TG-GCxSPIMS device, the limit of detection (LOD) is reduced. This can be deduced from the comparison of subsequent measurements applying both methods, TG-SPIMS and TG-GCxSPIMS. For the LOD calculation, the IUPAC definition,⁶⁸ with N as the averaged noise, S as the signal height, c as the concentration of an assayed substance, and σ as the noise variance, was applied:

$$\text{LOD} = \frac{2 \cdot \sigma}{|S - N|} \cdot c$$

For LOD determination, a standard mixture comprised of three alkanes (C_{10} , C_{12} , C_{17}) was used. Figure 4 shows two SPI mass spectra of heptadecane ($C_{17}H_{36}$). The mass spectrum in Figure 4B was recorded with the TG-GCxSPIMS device, whereas Figure 4A shows heptadecane measured without the separation step (TG-SPIMS). The GC oven temperature was held at 250 °C during the whole measurement. The acquisition frequency was set to 1 s

for both systems. Comparison between both spectra (A and B) demonstrates the benefit of the modulator, resulting in a higher signal-to-noise ratio. Subject to the condition that the concentration change of heptadecane is negligible during the acquisition time and the fact that C_{10} - and C_{12} -alkanes have already been evaporated at this time interval, the concentration of heptadecane could be calculated from the mass loss data of the thermobalance during the relevant cycle, considering the gas flow through the TG device of 60 mL min⁻¹. With the calculated concentration (c), the measured ion signal (S) at $m/z = 240$, and the noise variance (σ^2), a LOD for heptadecane of 2 ppm in case of TG-SPIMS and 210 ppb in case of TG-GCxSPIMS could be calculated. Note that the single photon ionization cross section of alkanes is up to 1 order of magnitude lower as compared to alkenes and aromatic compounds; in the latter cases, considerably lower values of LOD could be expected.

Using the modulator device involves two advantages, which will lead to an LOD improvement of TG-GCxSPIMS despite the lesser averaging. Because of the working principle of the modulator, substances are refocused to a sharp plug, which involves the entire sample evaporating during 30 s, before they are reinjected into the GC device. Consequently, the sample compounds are concentrated, while the noise level remains constant. This is

(68) Long, G. L.; Winefordner, J. D. *Anal. Chem.* **1983**, *55*, 712A–724A.

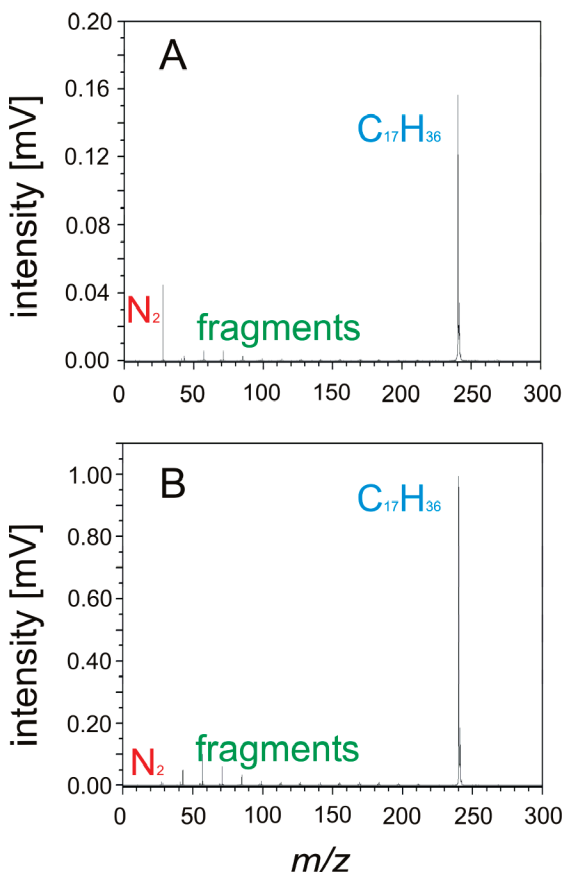


Figure 4. (A) SPI-TOFMS spectrum of heptadecane ($C_{17}H_{36}$) measured with TG-SPIMS. (B) SPI-TOFMS spectrum of heptadecane ($C_{17}H_{36}$) measured with TG-GCxSPIMS.

reflected in a higher signal-to-noise ratio, and, therefore, a lower LOD can be reached. Using controlled cold spots is a well-known technique for ultra trace analysis at the expense of temporal resolution. Furthermore, as compounds separate along the GC column, the level of so-called chemical noise that can be related to sample impurity can be reduced. The superposition of these two advantages leads in the end to an improved LOD in case of TG-GCxSPIMS as compared to TG-SPIMS.

Multi-Dimensional Data Space. With the extension of the TG-SPIMS approach by a GC separation, the two-dimensional plane shown in Figure 2B becomes a cube including retention times as additional dimension. Figure 5 illustrates such a three-dimensional (3D) TG-GCxSPIMS data set. The axes of the 3D space are defined as m/z , temperature of the TG furnace, and the GC retention time. For better clarity, only a couple of the molecular groups, for example, alkanes (black dots), cyclo-alkanes (yellow dots), benzene and methylated benzenes (green dots), indane and methylated indanes (cyan dots), and naphthalene and methylated naphthalenes (red dots), are displayed to explain the data structure. All these substances have been identified by the measurement of the diesel sample with a GCxGC-EIMS device. The different substances are presented as dots, wherein each dot represents the reinjection by the modulator during one modulation interval. The logarithmic intensity of the MS signals is represented by the size of these dots. The different colors demonstrate the corresponding chemical classes. For detailed investigation, different profiles can be derived from this data cube, which are

shown in Figure 5A–C. Figure 5A at the top exhibits the profile for one mass to charge ratio, here $m/z = 128$, whereas the X-axis is the TG-furnace temperature and the Y-axis is the retention time. This plot represents a sequence of modulated reinjections at different temperatures of the TG furnace. There are obviously two different compounds with $m/z = 128$, nonane (black dots) and naphthalene (red dots), which overlap in the m/z dimension. Because of the larger polarity of naphthalene as compared to nonane, the retention times differ from each other, and these two isobaric substances can be clearly separated with the presented setup. However, the temperature program of the GC oven (Table 1), which runs parallel to the temperature program of the TG oven, influences the retention behavior of the evolved substances on the GC column. In the case of nonane and naphthalene, the GC oven temperature program causes the retention time difference to decrease with time, that is, when going to higher TG oven temperatures. This can be clearly observed in Figure 5A.

To distinguish between isomeric molecules and compounds with identical molecular weight but different molecular structures (isobars), the m/z profile (Figure 5A) can be used. The different retention times as well as the different behavior of the retention times with rising temperature of the depicted compounds (nonane and naphthalene) are related to their different interaction with the stationary phase. Consequently, the retention behavior of each substance could be used as an indicator to distinguish between molecular classes.

As was already mentioned, with the adoption of the modulator, eluents are trapped and released every 30 s, which is equivalent to a temperature rise of the TG furnace of 5 °C. Figure 5B (temperature plot, blue) represents one injection at a specific temperature ($T = 190$ °C). It shows the separation in two dimensions due to the m/z ratio of each substance and the respective retention time. The chemical class-dependent retention of the molecules, which is similar to that of a GCxGC run, is clearly provided. For thermal analysis, the TG and DTG curves represent the change of the sample mass due to the temperature rise. With the presented setup, the TG and the DTG curves can be correlated to a sequence of two-dimensional separation plots. Each profile represents one reinjection of the sample by the modulator to the GCxSPIMS device. That means that for every change of the sample mass in a 30 s interval, a clearer evolved gas composition is given by a two-dimensional plot, whereas TG-SPIMS provides only a mass spectrum. Therefore, this depiction (m/z vs retention time, Figure 5B) gives additional information regarding thermal decomposition analysis.

Depending on the sample nature, TG can also be regarded as a separation technique in very special cases. In general, samples with components having a boiling temperature less than their decomposition temperature, for example, fuels or oils, show a temperature-dependent volatility and can be separated by distillation. This behavior is reflected in the retention time layer ($m/z-T$ layer, Figure 5C, green layer), where X-axis is the m/z separation and Y-axis is the temperature of the TG furnace and therefore the separation due to the boiling point of the components. Compounds with a higher boiling temperature are in the range of higher temperatures, whereas highly volatile substances such as benzene and alkylated benzenes are located in the lower temperature regions. Regarding the cubic structure again, different

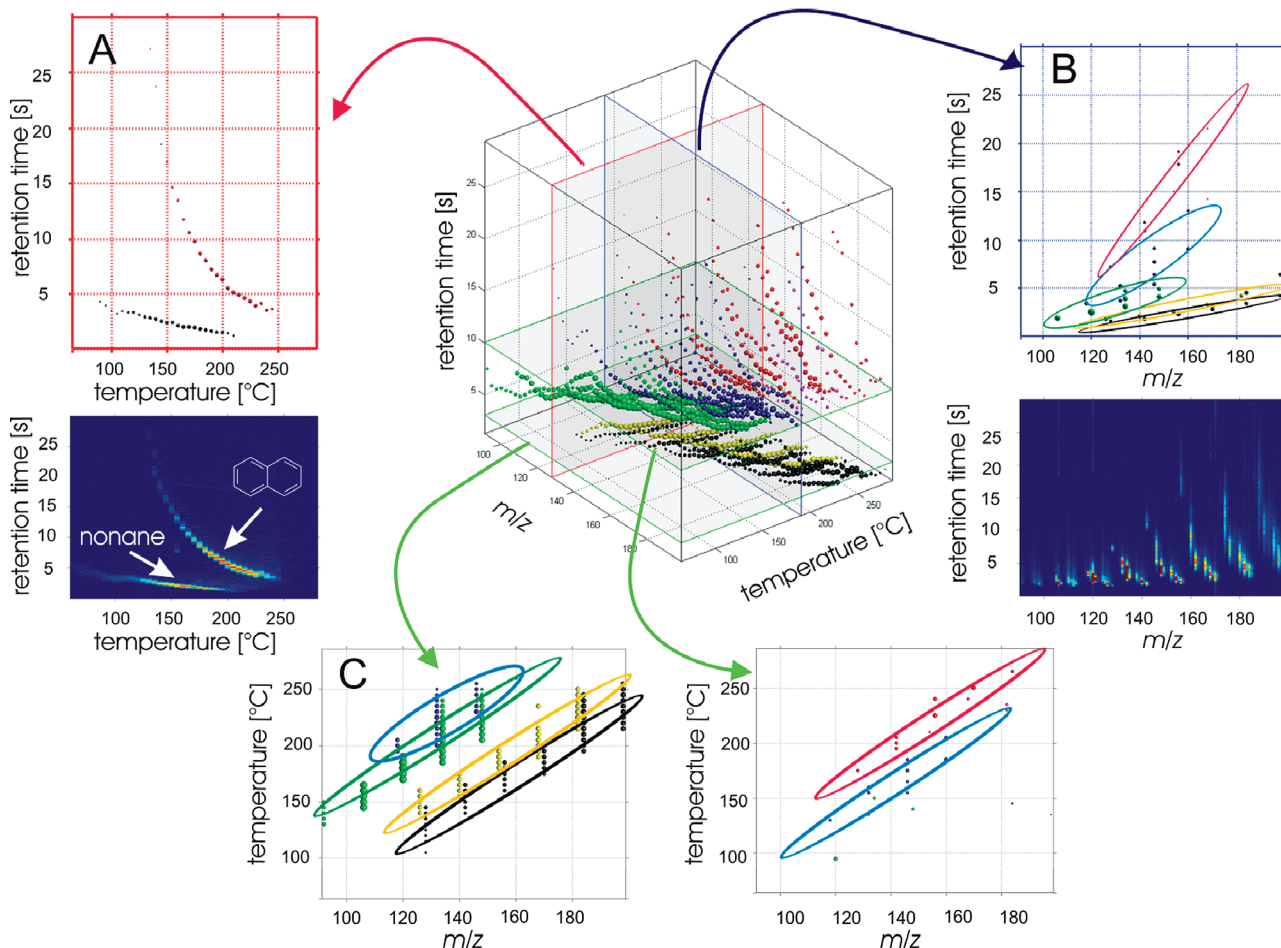


Figure 5. Representation of the three-dimensional data set (m/z vs temperature of TG oven vs GC retention time) obtained by TG-GCxSPIMS (center) and two-dimensional information derived from the data cube: (A) m/z profiles showing two species overlapping in m/z dimension, but clearly separated due to their different retention behavior as a function of TG oven temperature. (B) Temperature profiles representing one injection at a specific temperature ($T = 190$ °C), depicting retention time as a function of m/z . (C) Retention profiles showing TG oven temperature versus m/z : Compounds with a higher boiling temperature are in the range of higher retention times, whereas more volatile substances such as benzene and alkylated benzenes are located in the lower retention time regions.

Table 1. Temperature Program of the GC Oven

measurement	heating rate [°C/min]	time [min]	temperature [°C]
diesel fuel	0	0	40
	0	1	40
	30	2	100
	0	1	100
	10	2	120
	0	2	120
	8	15	240
	0	20	240
	-30	4	120
	0	15	120
	14	10	260
	0	50	260
	0	0	40
	0	2	40
ABS	10	3	70
	0	1	70
	10	5	120
	0	25	120
	10	14	260
	0	45	260

retention time intervals can be used to preselect the sample components due to their polarity, and to characterize them using

the m/z ratio and the boiling point information according to the compound location in the retention time layer. Sample substances with a high polarity are located at the top of the cube, whereas less polar compounds are positioned at the bottom. As mentioned, summation of all retention time layers will lead to the two-dimensional contour plot as is the case using TG-SPIMS and provide a simplified picture of the sample composition.

First Application. The novel TG-GCxSPIMS device was applied to analyze the thermal decomposition and evolved gaseous products of a common polymer, acrylonitrile-butadiene-styrene (ABS). Furthermore, LOD for toluene ($m/z = 92$) and styrene ($m/z = 104$) are determined.

ABS 011 P2MC Novodur. The ABS polymer (acrylonitrile, butadiene, styrene) is a copolymer made by polymerizing styrene and acrylonitrile in the presence of polybutadiene, resulting in long chains of polybutadiene grafted with side-chains of poly(styrene-acrylonitrile). Because of the bipolar nitrile groups, neighboring polymer chains attract each other, making ABS stronger than pure polystyrene.⁶⁹ The TG and DTG curves as well as SPI spectra of an ABS sample are depicted in Figure 6. The summed SPI

(69) Odian, G. *Principles of Polymerization*, 3rd ed.; John Wiley & Sons Inc.: New York, 1991.

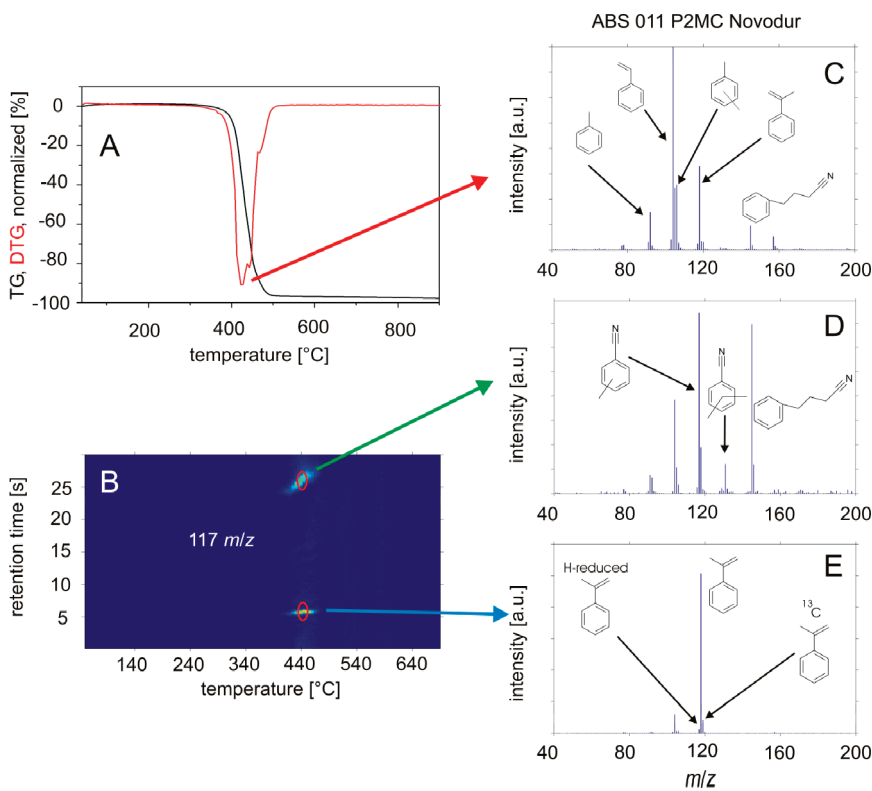


Figure 6. (A) TG and DTG curves of ABS blend. (B) Retention times of the eluents with $m/z = 117$ as a function of TG oven temperature. (C) SPI-TOFMS spectrum summed over all retention times at the temperature of maximum mass loss. (D,E) SPI-TOFMS spectra recorded at different retention times at the temperature of maximum mass loss.

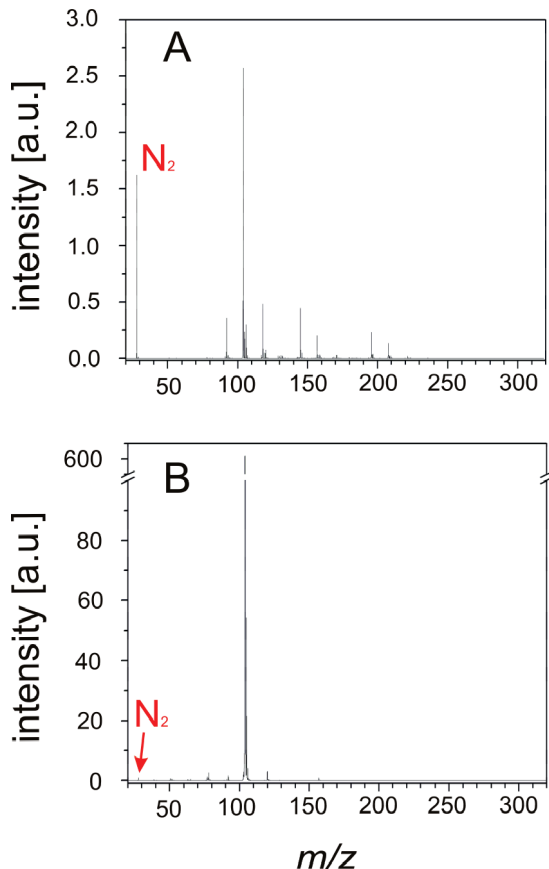


Figure 7. (A) SPI-TOFMS spectrum of ABS blend measured with TG-SPIMS. (B) SPI-TOFMS spectrum of ABS blend measured with TG-GCxSPIMS.

spectrum (30 s, Figure 6C) at the temperature of the maximum weight loss (440 °C) includes toluene ($m/z = 92$), ethylbenzene ($m/z = 106$), α -methylstyrene ($m/z = 118$), benzenebutanenitrile ($m/z = 145$), and benzene-C5-nitrile ($m/z = 157$), beside the main peak, styrene ($m/z = 104$).⁴⁵ Focusing on the α -methylstyrene signal, it shows an unusually high signal for dehydrogenated α -methylstyrene ($m/z = 117$) and consequently leads to the conclusion that there are overlapping peaks at $m/z = 117$. Figure 6B includes the corresponding m/z layer ($m/z = 117$) with two signals overlapping in the m/z axis but separated clearly along the retention time axis. It also shows two different retention time behaviors due to the unequal molecular structure of these two isobars, dehydrogenated α -methylstyrene and methylated benzonitrile. The two corresponding SPI mass spectra are pictured in Figure 6D and E. The mass spectrum (E) contains the α -methylstyrene signal and the expected isotope peak α -methylstyrene ($^{13}\text{C}-\text{C}_8-\text{H}_{10}$) beside the dehydrogenated α -methylstyrene ($m/z = 117$). Figure 6D, in contrast, contains the MS signals of benzenebutanenitrile ($m/z = 145$), benzenepropanenitrile ($m/z = 131$), and the methylated benzonitrile ($m/z = 117$), which are thermal fragments due to the decomposition of ABS. Because of the separation of these two species, a quantitative consideration of a mass of thermal fragmentation can be provided. Please note that the TG-SPIMS results cannot distinguish between thermal fragmentation and fragmentation due to the ionization process. TG-GCxSPIMS, in contrast, can provide results that lead to conclusions about the type of fragmentation due to the separation. Thermal fragment signals differ in their retention times, whereas fragmentation due to the ionization process has the same retention time as fragmentation takes place after

separation. That means two fragment signals with different retention times can only be assigned to thermal fragmentation.

Figure 7 represents mass spectra of pyrolyzed ABS recorded by TG-SPIMS and TG-GCxSPIMS at the temperature of maximal weight-loss. One benefit of the TG-GCxSPIMS method, the increased sensitivity due to the involved enrichment, is impressively demonstrated by the mass spectrum (B), where the intensity of the styrene monomer signal ($m/z = 104$) is more than 200 times higher than it is in case of TG-SPIMS (A). Two TG-GCxSPIMS mass spectra were used to determine the LOD for toluene ($m/z = 92$) and styrene ($m/z = 104$). A calibration standard gas containing 10 ppm of benzene, toluene, and *p*-xylene (BTX) was used for this purpose. The online measured signal intensity of 10 ppm toluene (not modulated) was used as standard. In case of styrene, the relative cross section of styrene as compared to toluene at 126 nm was used for quantification.³⁹ As described above, a LOD of 500 ppt for toluene and a LOD of 400 ppt for styrene were determined. Mühlberger et al.⁶¹ reported LODs for aromatic compounds measured with a comparable EBEL SPI-oaTOFMS setup in the range of 30 ppb. This is in good agreement with the expected improvement due to the enrichment character of the modulator device. Please note that the yield of the toluene signal in the TG-GCxSPIMS spectra is almost 200 times higher than it is in the case of direct TG-SPIMS, while the baseline variance sustains almost at the same level. This results in a significantly improved LOD as was shown for heptadecane in the previous section.

CONCLUSION

Thermal analysis (TA) coupled to soft single photo ionization mass spectrometry (SPIMS) is a powerful technology to reveal the complex composition of organic pyrolysis and vaporization products. In particular, through an innovative, bright electron beam pumped rare gas excimer VUV light source (EBEL), rather good detection limits are achievable. However, due to the vast complexity of pyrolysis gases, in many cases isobaric and isomeric molecules are not separable. This problem can be circumvented by implementation of a rapidly modulated gas chromatographic separation step between the thermal analysis device and the photo ionization mass spectrometer, as was realized in this work. This could be demonstrated by the analysis of hitherto undetected compounds in the evolved gases from the thermal degradation of ABS by TG-GCxSPIMS. Actually, this approach represents a semi comprehensive two-dimensional chromatographic-soft ionization mass spectrometric separation approach TG-GCxSPIMS. In addition to the largely increased selectivity, which, for example, allows the separation of isobaric alkanes and alkylated naphthalenes, also a significant reduction of the limit of detection is achieved.

ACKNOWLEDGMENT

Financial support by the BFS (Bayerische Forschungsstiftung) is gratefully acknowledged.

Received for review March 23, 2010. Accepted October 1, 2010.

AC100745H